

# Resolving Inconsistencies between Discretizations for the Density Operator and the Wigner Function

1<sup>st</sup> Alan Abdi 

Chair for High Frequency Techniques  
TU Dortmund

Dortmund, Germany  
alan.abdi@tu-dortmund.de

2<sup>nd</sup> Dirk Schulz 

Chair for High Frequency Techniques  
TU Dortmund

Dortmund, Germany  
dirk2.schulz@tu-dortmund.de

**Abstract**—This paper presents a comparison between two transport models used for quantum transport simulations, namely the conventional Wigner equation and a derived Wigner equation based on a two staggered grid formalism. The latter defines the Wigner function on two different grids, offset from each other. First results show that the two staggered grid formalism offers advantages over the conventional Wigner equation, particularly in terms of higher accuracy and in resolving the inconsistency, which is imposed by the correlation between the domains of the Wigner function and the density matrix.

## I. INTRODUCTION

The main focus of this study stems from the insightful discussions presented by Mains and Haddad [1] and Frenslley [2], who highlighted several constraints arising from the transformation between the discrete Wigner Function and the density matrix. These constraints can be summarized as follows:

1. The conventional Wigner function's domain does not coincide with that of the density matrix, posing a challenge in their direct correspondence.
2. A loss of half the information contained in the density matrix occurs during the Wigner-Weyl transformation.

These limitations can be attributed to two factors: the bounded computational domain and the uniform discretization employed [2]. In order to address these issues, a novel density matrix formalism is developed in this study, utilizing two distinct Wigner Functions defined on different grid points. The coupling between these functions is achieved and the information loss effectively eliminated. Notably, unlike Haddad's method, this approach assumes a common basis for the transformation into the phase space. Additionally, a Complex Absorbing Potential (CAP) is introduced as a complementary boundary condition in the  $\xi$ -direction, guaranteeing system stability. Consequently, the occurrence of negative charge carrier densities is prevented, and the challenges associated with boundary conditions appearing in [1] are successfully mitigated.

The subsequent section, section II, provides a concise derivation of the staggered grid formalism and establishes its relationship with the classical Wigner approach by employing a Taylor expansion. This theoretical foundation sets the stage for the numerical evaluation presented in section III. To

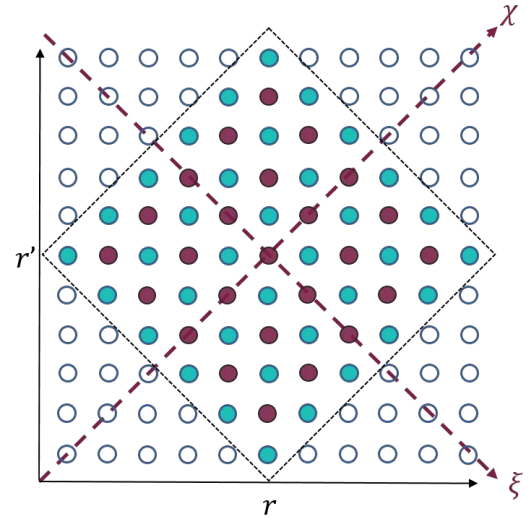


**Fig. 1:** Schematic of the staggered grid in center of mass coordinates before the basis transformation. The f grid is represented by the blue circles, while the g grid is represented by the red circles.

facilitate a comparative analysis, a resonant tunneling diode in an  $\text{Al}_{0.3}\text{Ga}_{0.7}\text{As}$ -GaAs material system is examined using both the newly proposed method and existing approaches e.g. the conventional Wigner Transport Equation (WTE) [3] and the Quantum Transmitting Boundary Method (QTBM) [4]. The latter is used as a reference method. By contrasting the outcomes, valuable insights can be gained regarding the effectiveness and accuracy of the novel density matrix formalism.

Finally, section IV presents a comprehensive conclusion that consolidates the findings of this study, highlighting the advantages of the proposed method over previous techniques.

## II. CONCEPT

First, a two dimensional discretization scheme with elements of the density matrix in real space and coordinates  $r$  and  $r'$  is assumed (Fig. 1). The elements are divided into two grids, which are offset from each other by  $|\Delta r|/2$ . The elements then are mapped onto the space domain  $(\chi, \xi)$  after a coordinate transformation with the center of mass coordinates  $\chi$  and  $\xi$  is applied. Afterwards, a basis transformation assuming plane

waves in  $\xi$ -direction is carried out according to [5] so that a representation in the phase space  $(\chi, k)$  results. The basis functions  $\Phi_f$  and  $\Phi_g$  which are used for the plane wave expansion are defined as

$$\Phi_f(\xi_f) = \sum_{k_l} \exp(-ik_l \xi_f) f_{\chi, k} \quad (1a)$$

$$\Phi_g(\xi_g) = \sum_{k_l} \exp(-ik_l \xi_g) f_{\chi_{mid}, k} \quad (1b)$$

with the wave numbers  $k$  as defined by

$$k = [-L_k/2, \dots, k_l, \dots, L_k/2] \Delta k, \quad (2)$$

where  $L_k$  is the number of  $k$ -values and  $\Delta k = \pi/(L_k \Delta x)$ .

As a result, transport equations for the Wigner functions  $f_{\chi, k}$  and  $f_{\chi_{mid}, k}$  related to both grids are derived and given by

$$i\hbar \frac{\partial}{\partial t} f_{\chi, k} = (\Phi_g^\dagger D_f \Phi_f) f_{\chi_{mid}, k} - (\Phi_f^\dagger V_f \Phi_f) f_{\chi, k} \quad (3)$$

and

$$i\hbar \frac{\partial}{\partial t} f_{\chi_{mid}, k} = (\Phi_f^\dagger D_g \Phi_g) f_{\chi, k} - (\Phi_g^\dagger V_g \Phi_g) f_{\chi_{mid}, k}, \quad (4)$$

where  $D_{f,g}$  is linked to the kinetic energy operator and  $V_{f,g}$  depends on the Hartree-Fock potential for each grid  $f$  and  $g$ , respectively. The index  $\chi_{mid}$  highlights the position of the second Wigner function  $f_{\chi_{mid}, k}$  in the  $g$ -grid, which is midway between the meshpoints  $\chi$  for grid  $f$  related to the Wigner function  $f_{\chi, k}$ . The relation to the classical Wigner formalism is shown with the help of Fig. 1. In this regard, a Taylor expansion is performed exemplarily at the grid point  $(\chi_0, \xi_0)$ . For demonstration purposes, the transport equation (3) in absence of the Hartree potential related term is given by

$$i\hbar \frac{\partial}{\partial t} f(\chi, \xi) = \frac{\hbar}{\Delta a_0^2 \cdot 2m^*} \cdot \left[ f(\chi_0 - \frac{1}{2} \Delta \chi, \xi_0 + \Delta \xi) + f(\chi_0 + \frac{1}{2} \Delta \chi, \xi_0 - \Delta \xi) - f(\chi_0 - \frac{1}{2} \Delta \chi, \xi_0 - \Delta \xi) - f(\chi_0 + \frac{1}{2} \Delta \chi, \xi_0 + \Delta \xi) \right], \quad (5)$$

where  $a_0$  represents the lattice constant of GaAs which here is defined as 0.563 nm. After carrying out the Taylor expansion, we arrive at

$$\frac{\partial}{\partial t} f|_{\chi_0, \xi_0} = \frac{\hbar}{\Delta a_0^2 \cdot 2m^*} \cdot \left( -2\Delta \chi \Delta \xi \frac{\partial}{\partial \chi \partial \xi} f|_{\chi_0, \xi_0} \right) + R. \quad (6)$$

The remainder  $R$  depends on monomials of  $\Delta \chi$  and  $\Delta \xi$ . Introducing the distances  $\Delta \chi = a_0/2$  and  $\Delta \xi = 2a_0$ , the relation  $\lim_{a_0 \rightarrow 0} R = 0$  holds. Hence, after taking the limit  $a_0 \rightarrow 0$ , we finally have

$$\frac{\partial}{\partial t} f|_{\chi_0, \xi_0} = -\frac{\hbar}{m^*} \cdot \frac{\partial}{\partial \chi \partial \xi} f|_{\chi_0, \xi_0}, \quad (7)$$

which is the Wigner equation at the grid point  $(\chi_0, \xi_0)$ . The application of this procedure onto (4) leads to the same result. Consequently, both transport equations (3) and (4) converge to the conventional Wigner equation if the distance between the sub-grids converges to zero.

Furthermore, the boundary conditions are supplemented by a CAP in  $\xi$ -direction to ensure that outgoing wavefunctions decay exponentially, preventing reflections at the boundaries of the  $\xi$ -domain [6], [7]. The basic concept behind a CAP is to add a complex-valued potential to the system's Hamiltonian before the basis transformation is carried out. Consequently, the matrices,  $V_f$  and  $V_g$ , related to the Hartree potential are extended by the CAP:

$$V_f(\chi, \xi) = V_f(\chi, \xi) - i\mathcal{C}_f(\xi). \quad (8a)$$

$$V_g(\chi, \xi) = V_g(\chi, \xi) - i\mathcal{C}_g(\xi). \quad (8b)$$

The complex potential causes the statistical density matrix within the layers to decay, reducing reflections at the computational domain's edges considerably. The complex absorbing potential can be efficiently constructed within the proposed formalism by a  $\xi$ -dependent monomial basis of the form:

$$\mathcal{C}(\xi) := \begin{cases} \beta \cdot (|\xi| - (\frac{L_\xi}{2} - \epsilon))^n, & \text{if } \frac{L_\xi}{2} - \epsilon < |\xi| < \frac{L_\xi}{2} \\ 0, & \text{elsewhere} \end{cases} \quad (9)$$

The width of the absorber is given by  $\epsilon$  and the coefficient  $\beta$  factorizes the amplitude of the complex potential. The exponent  $n$  is the third adjustable parameter and defines the monomial order of the CAP. Figure 2 shows the impact of the CAP on the system's stability with respect to the eigenvalue spectrum.

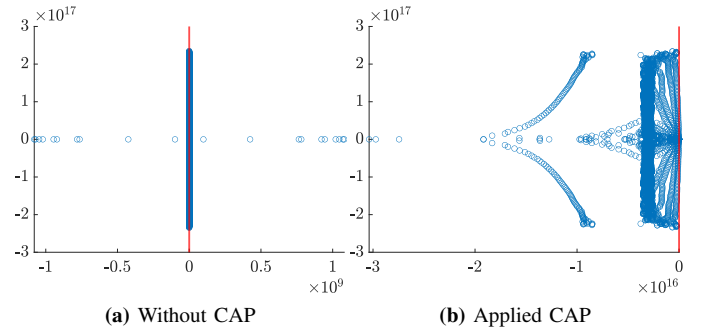


**Fig. 2:** Eigenvalues of the system matrix on the complex plane.

For demonstration purposes a relative small system matrix is considered with 3220 eigenvalues which corresponds to 81 cells in  $\chi$ -direction and 21 cells in  $\xi$ -direction. As can be seen from Fig. 2, an appropriate dimensioned CAP ensures that the eigenvalues are shifted to the left half plane. Once stability is achieved as a requirement, transient calculations can be performed as done in the upcoming section.

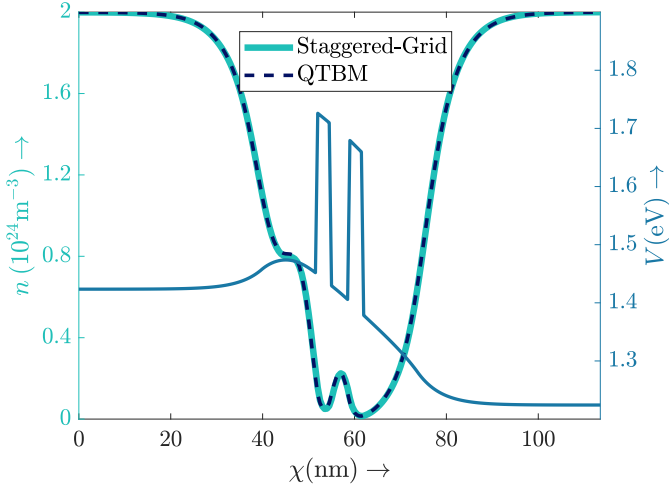


**Fig. 3:** Carrier densities  $n$  calculated with the staggered grid formalism and the classical Wigner method with an applied voltage of  $U = 0.2$  V.

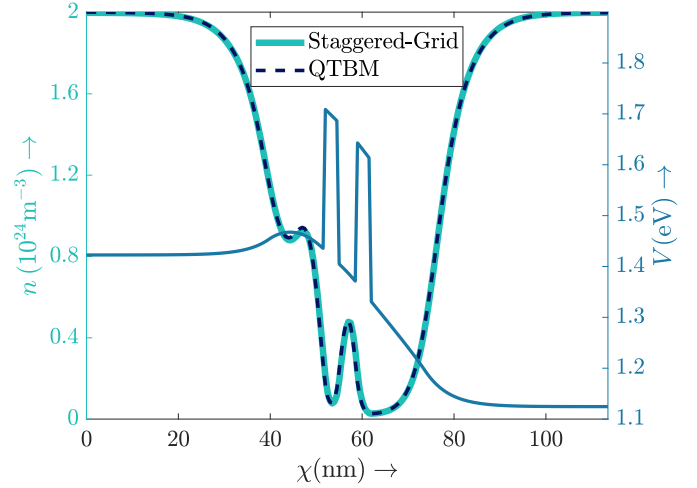


**Fig. 4:** Carrier densities  $n$  calculated with the staggered grid formalism and the classical Wigner method with an applied voltage of  $U = 0.3$  V.

### III. NUMERICAL EVALUATION

For the numerical evaluation a seven layer RTD, whose parameters are given in the Table I, is used as a test device. In addition, a spatially constant mass distribution ( $m = 0.063m_0$ ) and a one-dimensional transport in  $\chi$ -direction is assumed. Fig. 3 and Fig. 4 show the carrier densities for the new

**TABLE I:** Parameters of the RTD.

#Layer	1	2	3	4	5	6	7
Width (nm)	40	10	3	4	3	10	40
Doping ( $10^{18}\text{cm}^{-3}$ )	2	0	0	0	0	0	2
Potential (eV)	1.42	1.42	1.7	1.42	1.7	1.42	1.42

formalism and the QTBM in the self-consistent case. The self-consistent potential is obtained by coupling the transport equations with the Poisson equation. To address the corresponding nonlinearity, a standard Newton-Raphson method [8] is employed in all instances. The  $i$ -th iteration's stop criterion is specified as

$$\frac{\|V_H^i - V_H^{i-1}\|}{N_\chi} < 1 \cdot 10^{-3}, \quad (10)$$

where the vector  $V_H^i$  includes the  $N_\chi$  discretized Hartree potential values at the  $i$ -th iteration. The simulations for calculating the carrier densities were performed with the externally applied voltages 0.2 V and 0.3 V.

From Fig. 3 and Fig. 4, it can be concluded that the results from the proposed method (solid cyan line) agree very well with the results obtained from the reference method (black dashed line). For the evaluation, the discretization width of  $\Delta\chi = a_0$  is applied for both methods.

However, when it comes to the current-voltage characteristic, differences occur as it can be seen from Fig. 5 and Fig. 6. The Quantum Transmitting Boundary Method (QTBM)

serves again as an approved reference method. This time, the conventional Wigner transport equation is consulted to identify differences or similarities to the staggered grid formalism. For this purpose the absolute error  $\epsilon$  between both Wigner approaches and the QTBM is utilized as an indicator. The error between the staggered grid formalism and the QTBM is negligible for low voltages, when using a discretization width of  $\Delta\chi = a_0$  for all the three methods. On the other hand, if the discretization width is chosen so that the conventional Wigner method has a matrix as dense as that of the staggered formalism, the values of the current density  $j$  correspond to those of the reference solution and the error decreases. Hence, in Fig. 6 a discretization width of  $\Delta\chi = a_0/2$  is applied for the conventional Wigner method and the results show what goes along with the conclusions drawn from the Taylor Expansion in Section II. The results converge to the results of the reference solution. But the error overall between the Staggered Grid formalism and the QTBM is still notable smaller than the error between the QTBM and the classical Wigner method. This could be seen as an indication that the staggered grid formalism provides more accurate results.

In addition to the steady-state regime, the formalism presented here is now examined for the dynamic behavior. A transient simulation is carried out beginning with the system in thermal equilibrium  $t = 0$  fs. As an external bias of 0.1 V is applied, the system evolves towards a steady state and the statistical density matrix is reached under these conditions. The external bias is introduced through a time-dependent step function with an amplitude of 0.1 V. This evolution can be observed through the time-dependent behavior of the carrier density  $n$ , as demonstrated in Figure 7. For the time evolution, an explicit procedure, namely the fourth order Runge-Kutta method, is used.

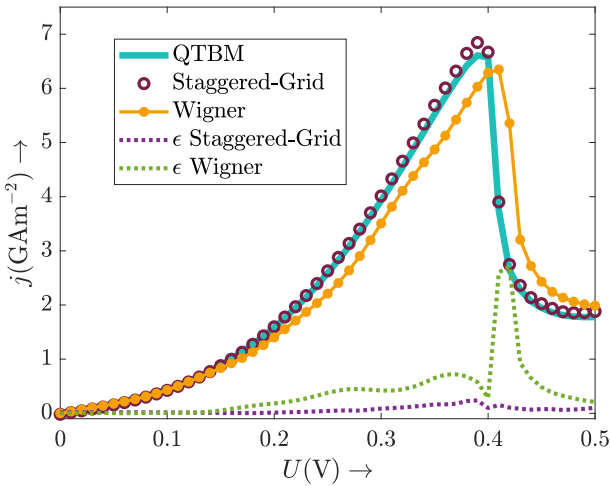


**Fig. 5:** I-V characteristic with a discretization width of  $\Delta\chi = a_0$  for the Wigner method. The absolute error  $\epsilon$  of the Staggered-Grid and the Wigner Equation to the QTBM is given.

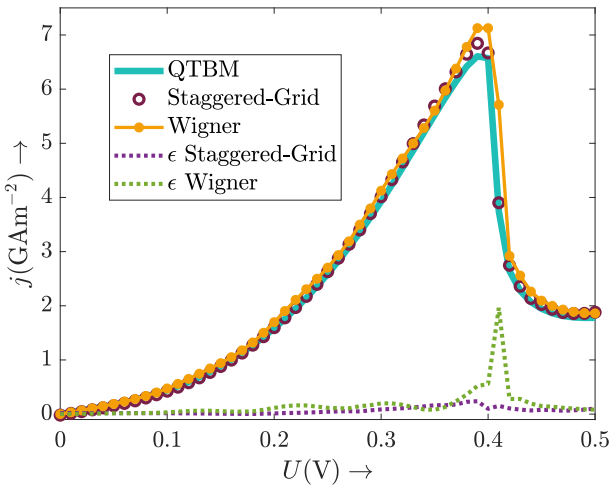


**Fig. 6:** I-V characteristic with a discretization width of  $\Delta\chi = a_0/2$  for the Wigner method. The absolute error  $\epsilon$  of the Staggered-Grid and the Wigner Equation to the QTBM is given.

#### IV. DISCUSSION AND CONCLUSION

Following the example of [1], the staggered grid formalism seems to be a promising approach because of its higher accuracy. In this work, previous limitations (occurrence of negative charge carrier densities and boundary conditions based on scattering terms) could be overcome by the successful implementation of a Complex Absorbing Potential and Plane Wave Expansion with the same basis with respect to the wavevector  $k$ . However, there are some challenges regarding the boundary conditions in  $\chi$ -direction since only one grid is physically located at the edge of the computational domain. The inflow and outflow concept was applied equally for both grids, leading to feasible results. Be that as it may, further investigation and the definition of new boundary conditions for the inner grid is needed here. The application of more accurate boundary conditions could improve the occurring deviations

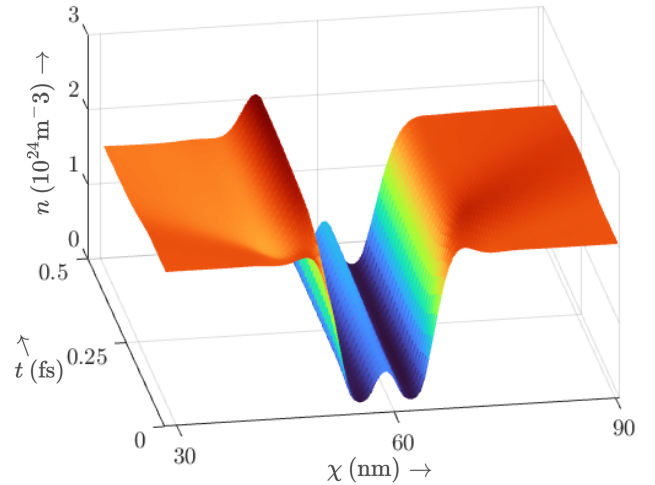


**Fig. 7:** Spatially time dependent carrier density  $n_f$ . The time step is chosen to be  $dt = 10^{-18}$ s.

from conventional methods at higher voltages as it can be seen from Fig. 5 and Fig. 6. The staggered grid formalism has a significant advantage over the traditional Wigner method in so far as it provides for an atomistic view of the materials used, allowing the tight binding concept to be introduced [9]. Increased accuracy and computational efficiency should result. Finally, this study demonstrates the potential of the two staggered grid formalism and establishes a relation to the conventional Wigner method.

#### ACKNOWLEDGMENT

This work was supported by the Deutsche Forschungsgemeinschaft DFG under Grant SCHU 1016/8-3.

#### REFERENCES

- [1] G.I. Haddad, and R.K. Mains, "An Accurate Re-formulation of the Wigner Function Method for Quantum Transport Modeling," *Journal of Computational Physics*, vol. 112, pp. 149–161, May 1994.
- [2] W. Frensky, "Boundary conditions for open quantum systems driven far from equilibrium," *Review of Modern Physics*, vol. 62., 745, July 1990.
- [3] J. Weinbub, and D. Ferry, "Recent advances in wigner function approaches", *Applied Physics Reviews*, Oct. 2018.
- [4] Craig S. Lent, and David J. Kirkner, "The quantum transmitting boundary method", *Journal of Applied Physics*, May 1990.
- [5] L. Schulz, B. Inci, M. Pech, and D. Schulz, "Subdomain-based exponential integrators for quantum Liouville-type equations," *Journal of Computational Physics*, vol. 20, pp. 2070–2090, October 2021.
- [6] L. Schulz, and D. Schulz, "Complex Absorbing Potential Formalism Accounting for Open Boundary Conditions Within the Wigner Transport Equation," *IEEE Transactions on Nanotechnology*, vol. 18, pp. 830–838, August 2019.
- [7] L. Schulz and D. Schulz, "Numerical Analysis of the Transient Behavior of the Non-Equilibrium Quantum Liouville Equation," in *IEEE Transactions on Nanotechnology*, Nov. 2018.
- [8] B. A. Biegel and J. D. Plummer, "Comparison of self-consistency iteration options for the Wigner function method of quantum device simulation", *PhysRevB*.54.8070, Sep. 1996.
- [9] A. Abdi, M. Pech, and D. Schulz, "Incorporation of the Tight Binding Hamiltonian into Quantum Liouville-type Equations", *International Workshop on Computational Nanotechnology (IWCN)*, Feb. 2023, ISBN: 978-84-09-51107-5.